On the thermodynamic stability of a charged arginine side chain in a transmembrane helix

Sudha Dorairaj and Toby W. Allen*

Department of Chemistry, University of California, One Shields Avenue, Davis, CA 95616

Edited by Ramón Latorre, Centro de Estudios Cientıficos, Valdivia, Chile, and approved January 11, 2007 (received for review November 26, 2006)

Biological membranes consist of bilayer arrangements of lipids forming a hydrophobic core that presents a physical barrier to all polar and charged molecules. This long-held notion has recently been challenged by biological translocon-based experiments that report small apparent free energies to insert charged side chains near the center of a transmembrane (TM) helix. We have carried out fully atomistic simulations to provide the free-energy profile for moving a TM helix containing a protonated Arg side chain across a lipid bilayer. Our results reveal the fundamental thermodynamics governing the stability of charged side chains in membranes and the microscopic interactions involved. Despite local membrane deformations, where large amounts of water and lipid head groups are pulled into the bilayer to interact with Arg, the free-energy barrier is 17 kcal/mol. We provide a rationale for the differences in our microscopic free energies and cell biological experiments using free-energy calculations that indicate that a protonated Arg at the central residue of a TM helix of the Leader peptidase might reside close to the interface and not at the membrane center. Our findings have implications for the gating mechanisms of voltage-gated ion channels, suggesting that movements of protonated Arg residues through the membrane will be prohibited.

Biological membranes are complex dynamical structures consisting primarily of a bilayer arrangement of phospholipid molecules in which hydrocarbon chains are segregated away from the aqueous phase to form a sheet-like nonpolar core region that is unfavorable to all polar and charged species (1). The properties of this membrane core play an essential role in providing a physical barrier that protects the cell from the environment, which is necessary to maintain membrane protein stability and function.

Charged protein side chains play important roles in several biological functions, including: protein folding (2), enzyme activity (3), nuclear localization (4), protein-mediated membrane fusion (5), protein–DNA interactions (6), pH activation of proteins (7), proton transport (8), and the voltage sensitivity of ion channels (9). The positioning of these residues within membrane proteins is driven by both their functional roles and interactions with the host membrane. As a result of the dehydration barriers that would be faced if these side chains were to enter the hydrophobic core of the membrane, they are found near or outside the membrane interface (10, 11). Theoretical estimates of the barrier faced by arginine, for example, based on a simplified picture of a rigid continuum dielectric membrane, are as high as 40 kcal/mol (12, 13) [see supporting information (SI) *Text* and SI Fig. 7].

This long-held view has recently been challenged by cell biological experiments that report apparent free energies for insertion of hydrophobic segments (H-segments) on the Leader peptidase (Lep), from *Escherichia coli*, by the translocon in the endoplasmic reticulum (14). Surprisingly, these experiments indicate that there is very little free-energy penalty (~2.5 kcal/mol) to include an Arg residue in the middle of an H-segment. One possible interpretation of these results is that Arg will face a small barrier to physical motion across the membrane. If this is the case, it suggests that all polar and charged species may easily cross the membranes that protect cells, opposing the prevailing view of membrane biophysics.

Translocon-based measurements represent an important advance, uncovering the thermodynamics governing sequence-dependent insertion during the synthesis of membrane proteins. However, these observations emerge from a complex biological system where the local partitioning environment remains uncharacterized. The Lep protein may remain associated with the translocon complex during detection by glycosylation, with polar faces of the H-segment shielded from lipid (14), and may subsequently reside in a region of perturbed (possibly thinned) membrane. In addition, the Lep protein itself consists of two more transmembrane (TM) segments that contain polar and charged side chains that could stabilize the H-segment (15). A further complication is associated with the undetermined protonation states of titratable residues in a membrane environment, in light of recent experimental evidence for significant pK_a reduction in nonaqueous environments (16). Despite these uncertainties, interpretation in terms of spatially resolved free energies, required if they are to be used to understand membrane protein conformational changes, hinges on the ability of the engineered sequence to "lock in" the H-segment across the bilayer. Given observations with the glycosylation mapping technique that TM helices can slide when charged side chains are attached (11), this lock-in ability should be examined.

The thermodynamic stability of charged side chains in membranes also has implications for our understanding of the mechanisms of voltage-gated ion channel activity. One proposed gating model involves large "paddle"-like motions of lipid-exposed protonated Arg side chains through the bilayer upon membrane depolarization (17, 18). Theoretically, the energetic cost of these conformational changes has been estimated to be as high as 265 kcal/mol (19). The paddle model suggests a very different mechanism to the conventional picture of voltage sensing that sequesters gating charges from lipid by protein (20, 21). Taken together with the translocon-based assay, we have good cause to revisit the theoretical description of charged residue–membrane interactions by using modern computational tools that treat the membrane in full dynamic and atomic detail.

Although the translocon experiments and the paddle model of ion channel gating provided the original impetus for this present work, we decided to address this problem in a more general fashion by using a single-model TM helix, as has been successful for studying protein–lipid interactions in recent years (22), and report the free-energy profile of an Arg side chain across a membrane. This knowledge will provide the key ingredient to understanding all biological processes that involve charged side-chain movement in membranes. We show that Arg does experience a large barrier and

Author contributions: T.W.A. designed research; S.D. and T.W.A. performed research; T.W.A. contributed new reagents/analytic tools; S.D. and T.W.A. analyzed data; and S.D. and T.W.A. wrote the paper.

The authors declare no conflict of interest.

This article is a PNAS direct submission.

Abbreviations: H-segment, hydrophobic segment; Lep, Leader peptidase; MD, molecular dynamics; PMF, potential of mean force; TM, transmembrane; COM, center of mass.

*To whom correspondence should be addressed. E-mail: tallen@chem.ucdavis.edu.

This article contains supporting information online at www.pnas.org/cgi/content/full/0610470104/DC1.

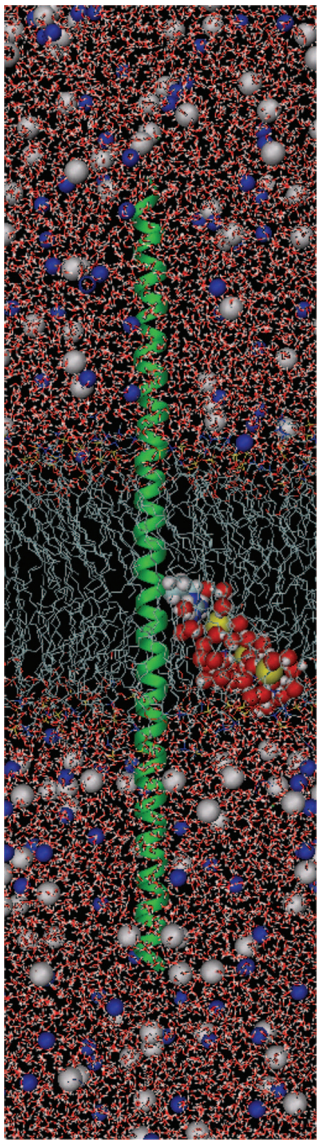

Fig. 1. TM helix system of 31,593 atoms. An 80-residue polyLeu α-helix (green) with neutral N (bottom) and C (top) termini and a central Arg (gray/cyan/white) spans a dipalmitoylphosphatidylcholine bilayer with 0.5 M KCl baths, containing 7,895 water molecules (red/white sticks), 72 K^+ (blue balls), and 73 Cl^- (gray balls) ions. Water and P atoms near Arg are shown as red/white and yellow balls, respectively.

present calculations to explain the small apparent free energies in biological experiments.

Results

Free Energy of an Arg Side Chain in a Membrane. Using molecular dynamics (MD) simulations described in *Theory and Methods*, we have calculated the potential of mean force (PMF) of a TM helix containing a central Arg side chain across a dipalmitoylphosphatidylcholine membrane. We have constructed a well defined model system (shown in Fig. 1) designed to separate out a common structural element of membrane proteins, the TM α-helix. This helix is approximately translationally invariant as a background polyLeu helix, such that when a central Arg residue is included, the resulting PMF will isolate the free energy of that side chain as a function of its position relative to the membrane.

The PMF (shown in Fig. 2) increases as Arg enters the bilayer, exhibiting little attraction to the interface, in accordance with

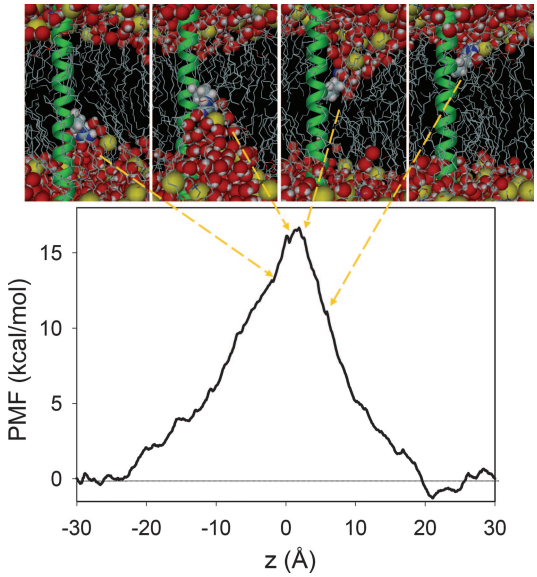

Fig. 2. PMF for the polyLeu+Arg TM helix (*Lower*), and MD snapshots when Arg is within the membrane core (*Upper*).

experiment (22, 23), then rises sharply to a maximum of 17 kcal/mol near the membrane center, suggesting that movement of an Arg side chain into the membrane core will be prohibited. As a result of careful sampling methods discussed in the next section, the PMF is well converged (see *SI Text* and SI Fig. 8) and is fairly symmetric on either side of the membrane.

Fig. 2 *Upper* reveals that the membrane does not maintain a uniform slab structure, as imagined in continuum models, instead undergoing local distortions as a result of water and head-group penetration. Despite coordination by water and head groups, the membrane cannot match the bulk aqueous-phase Arg hydration free energy [−60 kcal/mol (24)], leading to a significant barrier. Although "snorkeling" of basic side chains to the interface (25, 26) and head-group and water rearrangement (27) have been observed previously, Fig. 2 shows interfacial connections that require more substantial changes in local bilayer structure. These perturbations will incur strain energies that can help account for the sharp increase in free energy.

In fact, any conformational change of a protein requiring movement of the side chain from outside the membrane interface to the edge of the hydrophobic core ($|z| \sim 13$ Å) must overcome an average force of ~0.5 kcal/mol per Å. In the context of voltage-gated ion channel gating, this process would require TM potentials of the order of 0.5 V. The increased steepness of the PMF inside the core (~1 kcal/mol per Å) means that to push the Arg to the membrane center would require ~1 V, being an order of magnitude greater than physiological values.

We want to understand the origins of the shape and magnitude of this PMF. We have shown in *SI Text* that Arg remains coordinated by one lipid head group and four to five water molecules throughout the membrane (see SI Fig. 9). We note that Cl^- ions, like lipid carbonyls, do not play major roles in stabilizing the charge; yet they are not completely excluded from the membrane. The side chain experiences strong attractive interactions with lipid head groups and water throughout the membrane (of magnitude ~100 and 50 kcal/mol, respectively), providing a large driving force to pull polar groups into the core. Despite these attractive interactions, Fig. 2 tells us that the helix is, in fact, at its free-energy maximum; highly unstable when Arg is inside the membrane. Thus, although interesting, interaction energies are not free-energy contributions, and thus do not solely govern stability. They lack the multitude of interactions between peptide, lipids, and electrolyte (including the

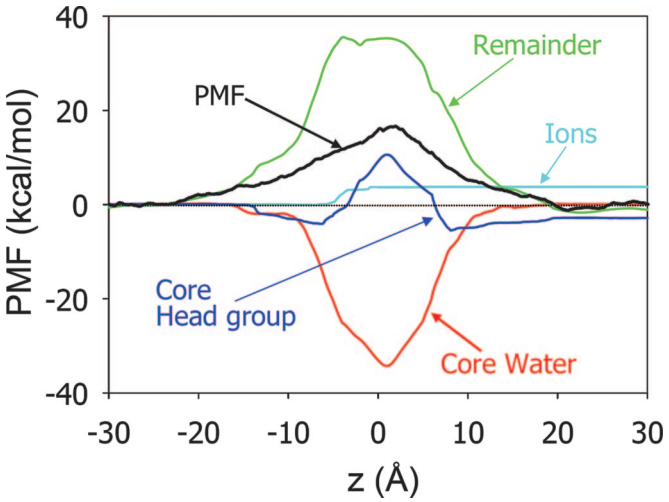

Fig. 3. Free-energy contributions from water (red), head groups (blue), and ions (cyan) drawn into the bilayer core. The black curve is the total PMF, and the green curve is the remainder after subtracting core group contributions.

strain energy needed to deform the membrane) and entropic contributions. To find the free-energy contributions, we invoke the relationship between the PMF, $W(z)$, and the mean force (Eq. **3**) to decompose the PMF into contributions, α (28),

$$W_\alpha(z) = W_\alpha(z') - \int_{z'}^{z} d\zeta \, \langle F_\alpha(\zeta) \rangle. \qquad [1]$$

where F_α is the instantaneous force acting on the helix center of mass (COM) due to component α. Contributions from polar (lipid head groups and water molecules) and ionic components that have entered within the core of the membrane ($|z| \leq 13$ Å based on water O, lipid P atoms, and ions) are considered to be most interesting. It is these groups that have altered the PMF from what one may predict for a uniform slab, to that shown in Fig. 2, and are important for understanding how the perturbed membrane is helping to stabilize the charge. Fig. 3 shows these contributions that vanish outside of the core because of exclusion of interactions with interfacially located groups, with small asymmetries of a couple of kcal/mol owing to careful sampling discussed in the next section. Core water, head groups, and ions stabilize the helix by as much as ~35, 5, and 3 kcal/mol, respectively. Remarkably, the core-water contribution is stronger by 35 kcal/mol near the membrane center, made possible by increased water penetration with side-chain depth, the large dipole moment of water, and its ability to stabilize charge in the gas phase (29). In contrast, despite the side chain remaining coordinated by one phosphate group, the core-head groups contribute ~15 kcal/mol less near the membrane center relative to the interface, actually causing a destabilization (positive PMF contribution) there. This destabilization can be understood in terms of the significant (hidden) strain energy associated with the bilayer deformations necessary to allow Arg–head-group interaction. These hidden contributions enter through the total potential energy in the configurational integrals for the mean forces (see *SI Text*). Thus, even if the Arg–head-group interaction is fairly constant, bilayer strains lead to a destabilizing contribution to the PMF. On the other hand, we expect that water molecules can effectively stabilize the charge with less indirect cost.

The remainder curve of Fig. 3 represents everything else that contributes to the PMF. If one subtracts from the total PMF (Fig. 3, black curve) all contributions from charged and polar moieties within the core, one is left with the Born dehydration (from interactions with bulk electrolyte and lipid hydrocarbon, estimated

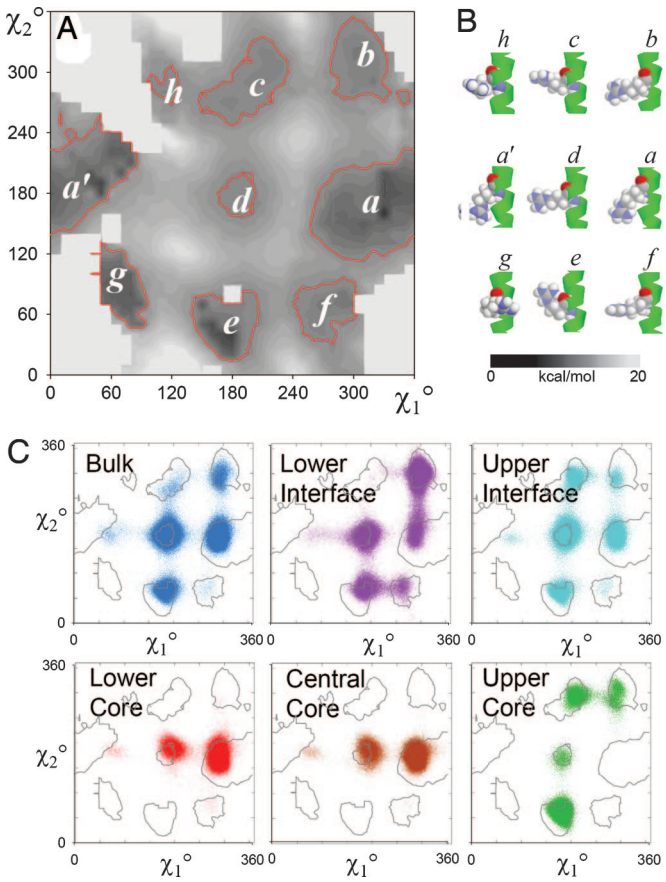

Fig. 4. Side-chain structural isomers. (*A*) Adiabatic energy map for an Arg side chain. Low energy states are labeled *a–h*. (*B*) The structures in *A* are illustrated. (*C*) MD rotamer distributions for Arg in the bulk ($|z| > 22$ Å), lower interface ($-22 \leq z < -13$ Å), upper interface ($13 < z \leq 22$ Å), lower core ($-13 \leq z < -4$ Å), central core ($-4 \leq z < 4$ Å), and upper core ($4 \leq z < 13$ Å).

to be 15–25 kcal/mol) plus interactions with the membrane interfaces [14–19 kcal/mol, assuming dipolar potentials of 600–800 mV (30, 31)]. The fact that the barrier in the overall PMF is 17 kcal/mol is a result of lipid and water PMF contributions being insufficient to overcome this substantial (~35 kcal/mol) electrostatic barrier presented by the membrane.

Role of Side-Chain Orientation. The problem of studying a side chain attached to a helix is more complicated than that of a simple side-chain analog, owing to the peptide's influence on the membrane and solvent, interactions with the peptide and the associated structural isomers of the side chain. The adiabatic energy map of Fig. 4*A* provides a guide to the accessible Arg rotamers, based on its first two dihedrals (χ_1 and χ_2). There are eight low-lying states (labeled *a-h* in Fig. 4*A*), with rotamer *a* the lowest in energy (by 2.0 kcal/mol), in accord with rotamer libraries (32), so it was chosen as the initial state for all simulations. This rotamer has its guanidine carbon directed downward toward the N terminus (and toward the lower interface when inside the membrane), as shown in Fig. 4*B*. Whereas the other rotamers are directed mostly away from the helix, rotamer *e* (second lowest in energy) also plays an important role because it is directed upward (toward the C terminus and the upper interface when inside the membrane).

The Ramachandran plots of Fig. 4*C* show 1.5 million instantaneous MD side-chain dihedral angle pairs to illustrate the relative stability and extent of isomerizations in different regions. When Arg is positioned in bulk solution, a wide spread of rotamers with different orientations was observed, indicative of good sampling.

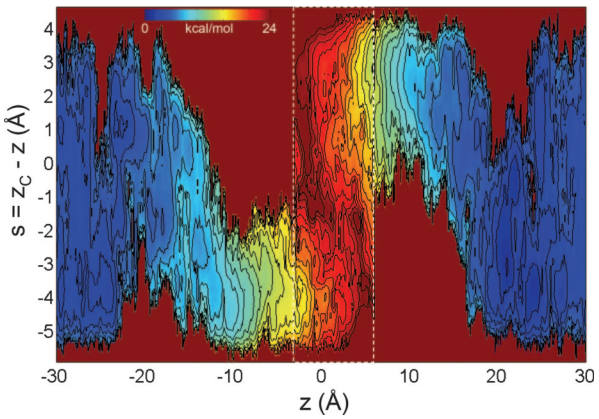

Fig. 5. 2D PMF as a function of helix position (z) and relative side-chain–helix position, $s = z_C - z$, obtained from a combination of 1D and 2D (dashed-box region) biased simulations.

This wide spread of orientations also exists at the interfaces, but with increased stability of outward-directed isomers (Fig. 4*A b*, *f*, and *c* in particular) caused by improved coordination by water and head groups when further from the helix. Inside the membrane core the distributions become restricted, being directed upward (Fig. 4*Ae*) in the upper core and downward (Fig. 4*Aa*) in the lower core. The images shown in Fig. 2 *Upper* revealed that, at some point near the membrane center, the side chain must "flip" to connect to the opposite interface. However, in the central core region the side chain has taken on a distribution not too dissimilar to that of the lower core, leading to a flip 4 Å above the membrane center (see SI Fig. 10). This off-center flipping suggests that either there is an inherent preference for the downward rotamer or that the strong forces (~10 kcal/mol per Å) pulling the side chain toward one interface or the other, create a barrier to isomerization that prevents an equilibrium distribution near the bilayer center. To overcome this challenge, we carried out additional 2D umbrella sampling simulations, biasing both the helix position, z, and relative side chain (guanidine C atom) position, $s = z_C - z$. The 2D PMF is shown in Fig. 5, with the additional 2D-biased simulation region indicated by a dashed box. In bulk water, the side chain uniformly samples all orientations ($-5 \le s \le 3$ Å). Near the interfaces ($z \sim \pm 20$ Å) the distribution narrows, with a preference for an outward-directed side chain. However, inside the core the side chain will be directed downward in $-13 \le z \le 1$ Å and upward in $1 \le z \le 13$ Å. This flipping close to (or just above) center signifies that the corresponding rotameric states are similar in free energy, with a slight preference for the downward-directed rotamer (as suggested by Fig. 4*A*). Off-center flipping can be attributed, in part, to the fact that the helix COM is coincident with the Arg C_α atom, but ~0.8 Å above the C_β atom.

At the bilayer center the barrier to flip the side chain is 4–5 kcal/mol. We anticipate low flipping rates caused by concerted motions of the side chain and lipid head groups and the low transverse (flip–flop) lipid diffusion (33). We have estimated the Kramer's transition rate for side-chain flipping in the high friction, large activation regime (34), using a measure of the diffusion coefficient for the side-chain relative position as described in *SI Text*. The flip rate was found to be 0.012–0.13 ns^{-1}, corresponding to a flip once every 10–100 ns and explaining the need for 2D biased simulations.

Having sampled an equilibrium distribution of both helix position and side-chain orientation, we integrated over the secondary variable, s, as shown in *SI Text*, to reveal the fairly symmetric 1D PMF of Fig. 2 and the contributions of Fig. 3. Although there are indications in Fig. 5 of regions of high free energy outside of the dashed box where the side chain will be directed away from the closest interface, these would contribute little to the final 1D PMF and its contributions.

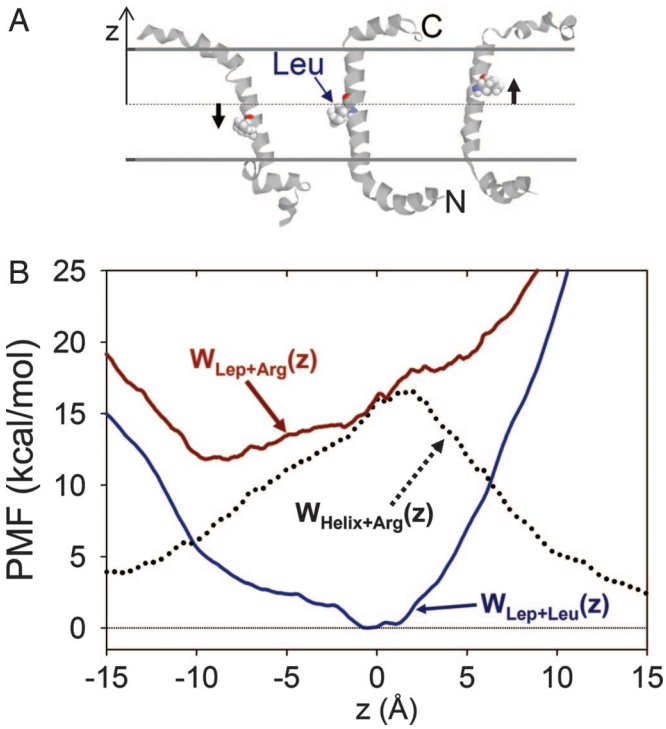

Fig. 6. Relating to translocon experiments. (*A*) Sample background helix (Lep+Leu) MD configurations. (*B*) Background Lep PMF (blue curve), polyLeu+Arg PMF from Fig. 2 (dotted black curve), and total PMF (Lep+Arg) (red curve).

Relation to Biological-Translocon Scale. How can we reconcile the 17 kcal/mol barrier to Arg motion through a membrane with the small 2.5 kcal/mol free energy from translocon experiments? Although there are several uncertainties in the complex biological system that may contribute to lower free energies, spatial interpretation hinges on the ability of the engineered H-segment to be locked tightly in a TM position. In these experiments, the Lep was engineered with an H-segment (19 Ala and Leu residues), flanked by Pro residues that prevent α-helix formation and thus considered to be excluded from the membrane core (where the polar backbone would experience a dehydration barrier). A sample of the 324 residues in the Lep sequence including the H-segment (bold) used for studying Arg based on information provided in ref. 14, is FEVPKNETKENGIRLSEGGPG**AAAALALALLLLALALAAAA** GPGGQPGQQLATWIVPPGQYF, which also contains polar and charged (on one side only) residues. We want to determine just how strongly would a protonated Arg side chain, placed at the central residue (underlined), be held near the membrane center. To answer this question, one must recognize that the protein will come to rest at the minimum in its free-energy surface that is governed by both the stability of the charged side chain in the membrane environment and the cost of displacing the background helix from its ideal TM orientation. We first estimate the PMF of the background Lep protein [$W_{Lep+Leu}(z)$] to ascertain the strength of the lock-in potential. We have chosen to estimate this PMF with a generalized Born implicit membrane (35), which adequately captures nonpolar and polar contributions to the energetics of protein–membrane interactions. Although the nature of the local membrane during Lep insertion is unknown, we chose a membrane mimicking a dipalmitoylphosphatidylcholine bilayer. Fig. 6*A* shows sample configurations after 10-ns simulations with the H-segment centered or

translated by ±5 Å. The resulting PMF is shown as a blue curve in Fig. 6*B*, converged to 0.06 kcal/mol. Indeed this lock-in potential is designed to hold the H-segment about the bilayer center (the PMF having a minimum there), but this well is not infinitely steep, rising by only 5 kcal/mol from $z = 0$ to -10 Å. To explore the robustness of the model, we also carried out calculations for a rigid TM helix with an unfolded peptide outside the H-segment, only to find a similar broad free-energy basin (see SI Fig. 11). However, just as a continuum membrane would overestimate the dehydration barrier for a charged residue (by tens of kcal/mol in the case of Arg), it also will overestimate that for polar backbone and side chains. Moreover, the conservative model membrane used was thicker (30 Å) and of lower dielectric constant (1) that even a purely saturated hydrocarbon core (~2). Thus the background lock-in potential may actually be considerably weaker than these results suggest.

The background PMF therefore provides only a small restoring force (~0.5 kcal/mol per Å or less) for large displacements. We then ask what would happen if the central residue was replaced by Arg. The large force imparted by the membrane on an Arg residue (~1 kcal/mol per Å), evident in Fig. 2, suggests that the Lep H-segment could be drawn far from its ideal TM position. Although the generalized Born approximation was adequate for analysis of the background helix, it should not be used for studying a charged residue. However, we show in *SI Text* that we may estimate the PMF for Lep containing a central Arg side chain by:

$$W_{\mathrm{Lep+Arg}}(z) \approx W_{\mathrm{Lep+Leu,\ GB}}(z) + W_{\mathrm{Helix+Arg,\ MD}}(z), \quad [2]$$

where $W_{\mathrm{Helix+Arg,\ MD}}(z)$ is the fully atomistic PMF for a polyLeu + Arg helix; in effect transforming a Leu into an Arg side chain. The result is a total PMF (red curve of Fig. 6*B*) that has a minimum at $z = -9$ Å. Although the value of this total free energy cannot be compared with experiment without a reference calculation for a non-TM configuration, this minimum tells us that the H-segment, hosting a central Arg residue, could slide to be accessible to the interface. Owing to the Lep sequence, this slide is toward the N terminus. We again emphasize that the actual lock-in potential could be considerably less steep, leading to even greater sliding. One can therefore expect an Arg placed at any residue in the H-segment to move to an interfacially accessible location and thus attain a similar apparent free energy. This free energy is expected to be dominated by the cost of translating the H-segment away from its perfect TM position (just a few kcal/mol) and not the free energy of the Arg as a function of its depth in the membrane (up to 17 kcal/mol).

Discussion and Conclusions

We have elucidated the free energetics governing the stability of a charged side chain in a membrane and have offered explanations for recent experimental results that oppose the long-held views of lipid-fearing charged residues. We have estimated that the work required to move a protonated Arg, attached to a TM helix, into the core of the membrane is as high as 17 kcal/mol.

This result has been obtained from ~μs fully atomistic–explicit solvent simulation to obtain an equilibrium distribution of helix positions across the membrane. These simulations revealed that the membrane is not a uniform slab, but perturbs significantly because of water and lipid head-group penetration when a charge is within its core. Indeed the Arg side chain is interacting favorably with water and head groups there, but not sufficiently to overcome the large dehydration barrier presented by the membrane and bilayer strain costs. A decomposition of the free energy revealed that, at the membrane center, only water effectively stabilizes the protein (by -35 kcal/mol). In contrast, lipid head groups drawn into the core present an overall destabilizing effect because of the cost of local bilayer deformations. These contributions explain the shape of the PMF, which rises steeply when the side chain cannot snorkel without lipid rearrangement.

Side-chain reorientations posed a challenge close to the bilayer center, leading us to undertake a 2D biasing of both helix positions and side-chain orientation. This 2D PMF revealed that downward and upward directed rotamers are similar in free energy near the bilayer center, but separated by a barrier of 4–5 kcal/mol, with flipping events occurring at the rate of one per 10–100 ns, prohibiting good sampling without additional bias. Integration of this 2D PMF yielded a 1D PMF with almost no asymmetry with maximum near the bilayer center. Simulation artifacts caused by finite membrane size and electronic polarizability were found to be small (≈1 kcal/mol; see SI Fig. 12), and *ab initio* calculations have been carried out to verify the accuracy of Arg–head-group and Arg–water interactions, demonstrating a representative configurational sampling of the true ensemble (see *SI Text*).

Although there may be several contributing factors in the translocon experiments, the small free energies observed for all residue types suggest that one's ability to engineer an H-segment that is locked in a TM configuration may be limited. Using additional simulations on the Lep protein we showed that the PMF responsible for holding the H-segment was not infinitely steep, instead increasing by only a few kcal/mol across the membrane core. Using a conservative model that maximized this restoring force, we estimated the PMF for an H-segment containing a central Arg, revealing that the H-segment could slide by 9 Å, allowing the side chain to snorkel to the interface. Such sliding is consistent with observations made with glycosylation mapping technique and does not prevent detection as TM because of the placement of glycosylation sites away from the H-segment. The inability of Lep to sufficiently anchor an H-segment can be understood in terms of the reported free energy as a function of the location of Pro (the residue chosen to lock in the TM helix) in the sequence, which varies by just ~1 kcal/mol (14). Then, the sliding of an Arg side chain placed within the H-segment can be understood because Born dehydration barriers for dipoles (e.g., the backbone) are less than those for monopoles (e.g., Arg).

Biophysical experiments based on the partitioning of amino acids or short polypeptides into "membrane-mimicking" substances (e.g., refs. 36–38), in particular *n*-octanol, have commonly been used to estimate the propensity for amino acids to enter the membrane core. Yet, the free energy to move an Arg side chain into *n*-octanol is a mere 1.5 kcal/mol (38), suggesting that this "nonpolar" solvent is nearly as efficient at stabilizing Arg as is water, with a large hydration free energy of -60 kcal/mol (24). Although partitioning into bulk solvents is clearly a simplified approximation for the heterogeneous lipid bilayer environment, this low free energy suggests that octanol cannot mimic the hydrocarbon core, which may be explained by the fact that saturated wet octanol contains 20–29 mol% water (39) and will lead to hydration of charges. The fact that there is fairly close correlation between octanol and interfacial hydrophobicity scales (40) (also ~1 kcal/mol for Arg) implies that octanol may be a better mimic for a membrane interface. Then, because the translocon scale also exhibits a good correlation with the octanol scale (14), one can be led to conclude that this biological scale reports the free energies of association with the interface and does not map out the free energy across the membrane, in support of the above Lep calculations.

Arg has a pK_a in aqueous solution of 12.5 (41), with corresponding deprotonation free energy of ~17 kcal/mol, and thus is typically assumed to be protonated, even in nonaqueous phase environments. However, recent experiments (16) have shown that the pK_a values of basic side chains drop by as much as 7 units when in a protein environment, leading us to postulate that similar shifts may occur inside the membrane. If so, the work required to deprotonate the side chain would be less than that to translate the protonated side chain to the membrane center. Such an outcome would indicate that the PMF governing Arg stability should be that of a neutral side chain deep inside the membrane core, creating a further complication when interpreting biological experiments.

The large barrier in the PMF suggests that protonated Arg movement in the membrane will be difficult, corresponding to membrane voltages of the order of 1 V, far greater than physiological values. Our findings therefore have implications for voltage-gated ion channel activity. It has been proposed that Arg residues, contained in each K channel voltage sensing S4 segment [4 or 5, which must remain protonated to explain observed gating charges (42)], move across the bilayer [by 15–20 Å (17, 18)] upon membrane depolarization, with some necessarily remaining lipid exposed. Although we have not simulated a voltage-gated K channel, or even an S4 segment, we have shown that Arg will face a large barrier to enter the membrane core, and we can anticipate even further destabilization if more than one Arg were to reside within the membrane core. MD simulations of an S4 segment of the KvAP channel in a bilayer (27) have suggested that S4 is stable as a TM helix, owing to attractive interactions with lipid head groups and water. Here, we have shown that strongly attractive interactions occur, even at the free-energy maximum, and thus cannot be used to draw conclusions about thermodynamic stability. The interaction of multiple Arg side chains with opposite interfaces (seemingly with no direction to slide) is likely to create a metastable state, and ultimately the helix must come to rest with all lipid-exposed Arg residues close to one interface. This idea offers a possible explanation for the low (+0.5 kcal/mol) free energy to insert an S4 segment in the translocon experiments (43). Our results therefore suggest returning to a more conventional picture of gating that protects charges from the lipid (20, 21) or to models that require modest Arg motions across a focused electric field (44, 45), supported by electron paramagnetic resonance and resonance energy transfer experiments (46, 47). Our results provide an important prediction that presents a challenge to experiments to match the quantitative thermodynamics and atomic-level understanding provided by these computer simulations.

Theory and Methods

MD can be used to reveal the average systematic force, $\langle F(z)\rangle$, that governs the thermodynamic equilibrium distribution along an order parameter, z. The free-energy profile, or potential of this mean force, $W(z)$, relative to some reference (z'), is:

$$W(z) - W(z') = -\int_{z'}^{z} d\zeta \, \langle F(\zeta)\rangle$$

$$= -kT \ln \frac{\int d^{3N-1}\,\mathbf{R}\, e^{-U(\mathbf{R}, z)/kT}}{\int d^{3N-1}\,\mathbf{R}\, e^{-U(\mathbf{R}, z')/kT}}, \qquad [3]$$

where k is the Boltzmann constant, T is the temperature, and U is the potential energy as a function of z and the $3N-1$ remaining coordinates, **R**. We have chosen our order parameter to be the position, parallel to the membrane normal, of the helix COM relative to the membrane COM. To assist sampling, harmonic biasing (or "window") potentials were added to the potential at regular intervals spanning the order parameter in the method of umbrella sampling (48). Trajectories were then unbiased postsimulation (49) to reveal the free energy along the coordinate, z.

PolyLeu was chosen as a suitable background TM helix (22), with 80 residues, spanning a length of ~120 Å. This helix can be translated within $-30 \le z \le 30$ Å without the (neutral) termini approaching the membrane interface. To avoid unfolding of the helix outside the membrane, which would require more configurational sampling that adds little to our knowledge of side-chain stability within the membrane, we applied dihedral constraints to maintain an approximately α-helical peptide. The helix was positioned at regular depths across the bilayer, and a new hydrated membrane was built around it for each position. Bilayers consisted of 48 dipalmitoylphosphatidylcholine molecules; chosen because it is the best-studied bilayer system and is a suitable model for a biological membrane. Each of 61 windows spanning $-30 \le z \le 30$ Å was equilibrated until side-chain interaction energies had converged, requiring up to 2 ns (see *SI* Fig. 10), followed by 5 ns for PMF calculation.

Additional multiple-bias simulations were used to thoroughly sample side-chain configurations. A 2D array of 110 windows, spanning a region near the membrane center ($-4 \le z \le 6$ Å) was built, equilibrated for 1.5 ns and then simulated for an additional 0.5–1 ns each. The 2D PMF, $W(z,s)$, emerging from 2D unbiasing (50), was then combined with a separate 2D PMF obtained from the z-only biased trajectories (spanning the entire membrane) via a simple relationship derived in *SI Text* and shown in SI Fig. 13.

We have calculated the PMF for the Lep protein (SWISSPROT ID code P00803) using the 61 residue sequence provided in *Results*, with standard N and C termini. We carried out an umbrella sampling calculation by using 31 windows (in 1-Å steps spanning $-15 \le z \le 15$ Å), each for 10 ns of Langevin dynamics simulation with a generalized Born implicit membrane (35). Simulation methods are described in more detail in *SI Text*.

We thank Benoit Roux for helpful suggestions, in particular for the understanding of connections to the reported translocon scale; Olaf Andersen, Roger Koeppe, and Nir Ben Tal for interesting discussions; and Igor Vorobyov for the *ab initio* calculations. This work was supported by National Science Foundation Career Award MCB-0546768 and in part by Pittsburgh Supercomputing Center Grant MCB050002.

1. Gennis R (1989) *Biomembranes: Molecular Structure and Functions* (Springer, New York).
2. Yang A-S, Honig B (1992) *Curr Opin Struct Biol* 2:40–45.
3. Huang HC, Briggs JM (2002) *Biopolymers* 63:247–260.
4. Kalderon D, Richardson WD, Markham AF, Smith AE (1984) *Nature* 311:33–38.
5. Han X, Bushweller JH, Cafiso DS, Tamm LK (2001) *Nat Struct Biol* 8:715–720.
6. Luscombe NM, Laskowski RA, Thornton JM (2001) *Nucleic Acids Res* 29:2860–2874.
7. Cuello L, Romero J, Cortes D, Perozo E (1998) *Biochemistry* 37:3229–3236.
8. Mathies RA, Lin SW, Ames JB, Pollard WT (1991) *Annu Rev Biophys Biophys Chem* 20:491–518.
9. Armstrong CM, Bezanilla F (1973) *Nature* 242:459–461.
10. Davis JH, Clare DM, Hodges RS, Bloom M (1983) *Biochemistry* 22:5298–5305.
11. Killian JA, von Heijne G (2000) *Trends Biochem Sci* 25:429–434.
12. Honig BL, Hubbell WL (1984) *Proc Natl Acad Sci USA* 81:5412–5416.
13. Kessel A, Ben-Tal N (2002) *Curr Top Membr* 52:205–253.
14. Hessa T, Kim H, Lundin C, Boekel J, Andersson H, Nilsson I, White SH, von Heijne G (2005) *Nature* 433:377–381.
15. Shental-Bechor D, Fleishman S, Ben-Tal N (2006) *Trends Biochem Sci* 31:192–196.
16. Cymes GD, Grosman C (2005) *Nature* 438:975–980.
17. Jiang Y, Ruta V, Chen J, Lee A, MacKinnon R (2003) *Nature* 423:42–48.
18. Ruta V, Chen J, MacKinnon R (2005) *Cell* 123:463–475.
19. Grabe M, Lecar H, Jan YN, Jan LY (2004) *Proc Natl Acad Sci USA* 101:17640–17645.
20. Hille B (2001) *Ionic Channels of Excitable Membranes* (Sinauer, Sunderland, MA).
21. Ahern CA, Horn R (2004) *Trends Neurosci* 24:303–307.
22. Killian JA (2003) *FEBS Lett* 555:134–138.
23. Wimley WC, Creamer TP, White SH (1996) *Biochemistry* 35:5109–5124.
24. Deng Y, Roux B (2004) *J Phys Chem B* 108:16567–16576.
25. Segrest JP, DeLoof H, Dohlman JG, Brouillette CG, Anantharamaiah GM (1990) *Protein Sci* 8:103–117.
26. Sankararamakrishnan R, Weinstein H (2000) *Biophys J* 79:2331–2344.
27. Freites JA, Tobias DJ, von Heijne G, White SH (2005) *Proc Natl Acad Sci USA* 102:15059–15064.
28. Roux B, Karplus M (1991) *Biophys J* 59:961–981.
29. Allen TW, Andersen OS, Roux B (2004) *Proc Nat Acad Sci USA* 101:117–122.
30. Smondyrev AM, Berkowitz ML (1999) *Biophys J* 77:2075–2089.
31. Stern HA, Feller SE (2003) *J Chem Phys* 118:3401–3412.
32. Dunbrack R, Karplus M (1993) *J Mol Biol* 230:543–574.
33. Marti J, Csajka FS (2003) *Europhys Lett* 61:409–414.
34. Crouzy S, Woolf T, Roux B (1994) *Biophys J* 67:1370–1386.
35. Im W, Feig M, Brooks CL (2003) *Biophys J* 85:2900–2918.
36. Radzicka A, Wolfenden R (1988) *Biochemistry* 27:1664–1677.
37. Wimley WC, White SH (1992) *Biochemistry* 31:12813–12818.
38. White SH (2003) *FEBS Lett* 555:116–121.
39. Sangster J ed (1997) *Octanol-Water Partitioning Coefficients: Fundamentals and Physical Chemistry* (Wiley, Chichester, UK).
40. Wimley WC, White SH (1996) *Nat Struct Biol* 3:842–848.
41. Cantor CR, Schimmel PR (1980) *Biophysical Chemistry: Techniques for the Study of Biological Structure and Function* (Freeman, San Francisco).
42. Schoppa NE, McCormack K, Tanouye MA, Sigworth FJ (1992) *Science* 255:1712–1715.
43. Hessa T, White SH, von Heijne G (2005) *Science* 307:1427.
44. Cha A, Snyder GE, Selvin PR, Bezanilla F (1999) *Nature* 402:809–813.
45. Chanda B, Asamoah OK, Blunck R, Roux B, Bezanilla F (2005) *Nature* 436:852–856.
46. Cuello LG, Cortes DM, Perozo E (2004) *Science* 306:491–495.
47. Posson DJ, Ge P, Miller C, Bezanilla F, Selvin PR (2005) *Nature* 436:848–851.
48. Torrie GM, Valleau JP (1977) *J Comp Phys* 23:187–199.
49. Kumar S, Bouzida D, Swendsen RH, Kollman PA, Rosenberg JM (1992) *J Comp Chem* 13:1011–1021.
50. Souaille M, Roux B (2001) *Comp Phys Commun* 135:40–57.